Since January 2020 Elsevier has created a COVID-19 resource centre with free information in English and Mandarin on the novel coronavirus COVID-19. The COVID-19 resource centre is hosted on Elsevier Connect, the company's public news and information website.

Talanta 258 (2023) 124466

Contents lists available at ScienceDirect

Talanta

journal homepage: www.elsevier.com/locate/talanta

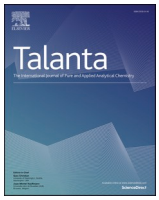

Hand-powered centrifugal micropipette-tip with distance-based quantification for on-site testing of SARS-CoV-2 virus

Chungen Qian [1], Jiashuo Li [1], Zheng Pang [1], Han Xie, Chao Wan, Shunji Li, Xin Wang, Yujin Xiao, Xiaojun Feng, Yiwei Li, Peng Chen [**], Bi-Feng Liu [*]

The Key Laboratory for Biomedical Photonics of MOE at Wuhan National Laboratory for Optoelectronics-Hubei Bioinformatics & Molecular Imaging Key Laboratory, Systems Biology Theme, Department of Biomedical Engineering, College of Life Science and Technology, Huazhong University of Science and Technology, Wuhan, 430074, China

ARTICLE INFO

Handling Editor: J.-M. Kauffmann

Keywords:
SARS-CoV-2
Immunoassay
POCT
Distance-based readout

ABSTRACT

This paper proposed a hand-powered centrifugal micropipette-tip strategy, termed HCM, for all-in-one immunoassay combined with a distance-based readout for portable quantitative detection of SARS-CoV-2. The target SARS-CoV-2 virus antigen triggers the binding of multiple monoclonal antibody-coated red latex nanobeads, forming larger complexes. Following incubation and centrifugation, the formed aggregated complexes settle at the bottom of the tip, while free red nanobeads remain suspended in the solution. The HCM enables sensitive (1 ng/mL) and reliable quantification of SARS-CoV-2 within 25 min. With the advantages of free washing, free fabrication, free instrument, and without the optical device, the proposed low-cost and easy-to-use HCM immunoassay shows great potential for quantitative POC diagnostics for SARS-CoV-2.

1. Introduction

The coronavirus disease 2019 (COVID-19) pandemic has become a severe global threat and is continuing to severely affect public health and the economy [1–3]. According to the World Health Organization (WHO), there are over 600 million confirmed cases and more than 6 million deaths by the end of September 2022. Considering its high infectivity rate, on-site, rapid, and early point-of-care testing (POCT) is particularly critical for timely isolation and intervention [4].

In terms of assay formats, severe acute respiratory syndrome coronavirus 2 (SARS-CoV-2) testing can be mainly carried out by nucleic acid-based molecular amplification and serum-based immunoassays [5–7]. In practice, classical quantitative assays, such as reverse transcription polymerase chain reaction/quantitative polymerase chain reaction (RT-PCR/qPCR) [8], enzyme-linked immunosorbent assay (ELISA), and chemiluminescence (CLIA), have played key roles for health monitoring during the outbreaks of COVID-19 [9,10]. However, the requirements of sophisticated equipment, specialized personnel, and multi-step processes have limited their potential application in POCT for on-site detection [11]. Alternatively, turbidimetric inhibition immunoassay (TIIA) was able to partially overcome the above-mentioned shortcomings, but still require optical detection equipment for quantification [12,13] (Fig. 1a).

Direct detection of SARS-CoV-2 antigens by lateral flow immunochromatography (LFIA) has been widely applied for preliminary large-scale screening due to its advantages of superior simplicity in operation and visualized detection, especially the in-home-self-testing scenarios could effectively reduce the risk of spreading during the epidemic by the mass gathering [14] (Fig. 1b). Considering the limitation of low sensitivity caused by the insufficient reaction between antigens and antibodies of conventional LFIA, Xu et al. recently reported a promising handheld microfluidic filtration platform for self-testing of the SARS-CoV-2 Virus [15]. The antigen-antibody binding was carried out within a test tube, enabling an immediate and synchronal contact of antigen- and antibody-conjugated beads and achieving a low detection limit of less than 100 copies mL^{-1} within 30 s. The detection signal was then obtained by the naked-eye reading of the red color intensity, which was potentially affected by subjective interpretation. Subsequently, to fulfill quantitative measurement while maintaining a simple and user-friendly interface, Wu et al. demonstrated a novel microfluidic chip

* Corresponding author.
** Corresponding author.
E-mail addresses: gwchenpeng@mail.hust.edu.cn (P. Chen), bfliu@mail.hust.edu.cn (B.-F. Liu).
[1] These authors contributed equally to this work.

https://doi.org/10.1016/j.talanta.2023.124466
Received 15 January 2023; Received in revised form 10 March 2023; Accepted 16 March 2023
Available online 18 March 2023

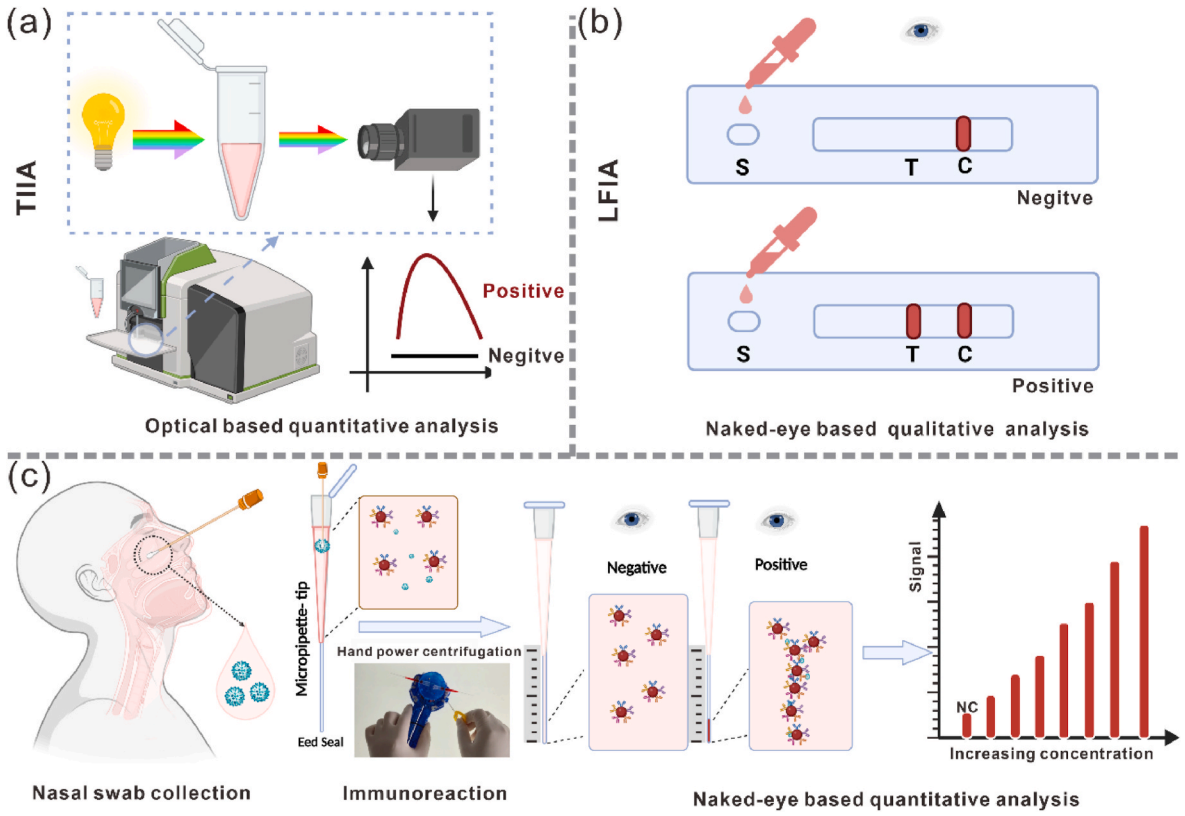

Fig. 1. Comparison of the three platforms. (a) Schematic diagram of TIIA. (b) Schematic diagram of LFIA. (c) Schematic diagram of HCM. NC stands for negative control.

with a particle dam for quantitative visualization of SARS-CoV-2 antibody levels from the accumulation length of the microparticles functionalized with antibodies [16]. However, despite promising progress, most of these POC platforms enable naked-eye qualitative detection or additional instrument-assisted quantitative detection. Thus, it is desirable to develop a low-cost, simple, instrument-free platform with quantitative visualization for POC diagnostics of SARS-CoV-2 [17].

Recently, distance-based signal readout, which does not need fluorescence or optoelectronic detector, has attracted increasing attention for biochemical sensing because of its potential capability of naked eye quantitative detection [18–23]. Additionally, compared to other instrument-free approaches, cost-effective and portable centrifugal toys have emerged as one of the most promising bio-analysis systems [24]. For example, inspired by historic whirligig (or buzzer) toys, Bhamla et al. first developed a hand-powered ultralow-cost paper centrifuge for plasma separation and malaria parasites isolating from whole blood [25]. Later, Michael et al. also described a custom-made fidget spinner for rapid on-site detection of urinary tract infections [26]. Given the above-mentioned factors, in this paper, we proposed a novel hand-powered centrifugal micropipette-tip (HCM) based platform that allows direct quantitative visualization of SARS-CoV-2 virus antigen levels (Fig. 1c). The centrifugal micropipette tip with an inner diameter of 300 μm is prepared by loading homogeneous immunoreaction reagents into a commercial long micropipette tip with the tip end sealed with epoxy glue to avoid liquid leakage during centrifugation (Fig. S1). The presence of the target SARS-CoV-2 Virus antigen can trigger the multiple monoclonal antibodies coated red latex nanobeads (200 nm) to bind together to form larger complexes of different sizes and shapes (Figs. S2a–d). After incubation at 37 °C and then centrifugation of the HCM, the formed aggregated complexes are settled in the bottom of the tip, while free red nanobeads will remain suspended in the solution because of their lower density. Finally, the concentrated nanobeads of different distances can be easily quantitatively read with the naked eye, without dependence on fluorescence or an optoelectronic detector, which will be one of the ideal solutions for point-of-care or self-service testing.

2. Results and discussion

To assess the feasibility of HCM, we first conducted a theoretical analysis. The sedimentation rate of spherical nanobeads is calculated by Stokes' law (Eqn (1)) [27]:

$$U_S = \frac{2(\rho_m - \rho_f)gR^2}{9\mu} \quad (1)$$

where *Us* represents the sedimentation velocity of the nanobeads, ρ_m is the density of the nanobeads, ρ_f is the density of the fluid, μ represents the fluid's viscosity, and g is the acceleration due to gravity or centrifugation, and R is the radius of nanobead. Eqn (1) indicated how this approach could be a simple but very effective method to separate aggregated complexes from unreacted nanospheres. The radius of the free unreacted nanosphere (200 nm) is significantly smaller than that of aggregated complexes (Figs. S2b–d). Theoretically, because of this size difference, the large complexes are pelleted quickly to the bottom of the tip, and free red nanobeads will remain suspended in the solution under suitable centrifugation conditions.

We have conducted three iterations of the proposed strategy to meet different application scenarios. Initially, as shown in Figure S3a-c, a home-made t ray was fabricated by a portable CO_2 laser cutter (Laser technology, China) with two (Polymethyl methacrylate) PMMA sheets (YoungChip, China) via a fast laser print, cut, and laminate (PCL) methodology [28]. As a proof of concept, six separate micropipette tips were successfully loaded and then tested simultaneously on a custom electric motor, demonstrating the great potential of high throughput. To further lower the application threshold, the experiments can be carried

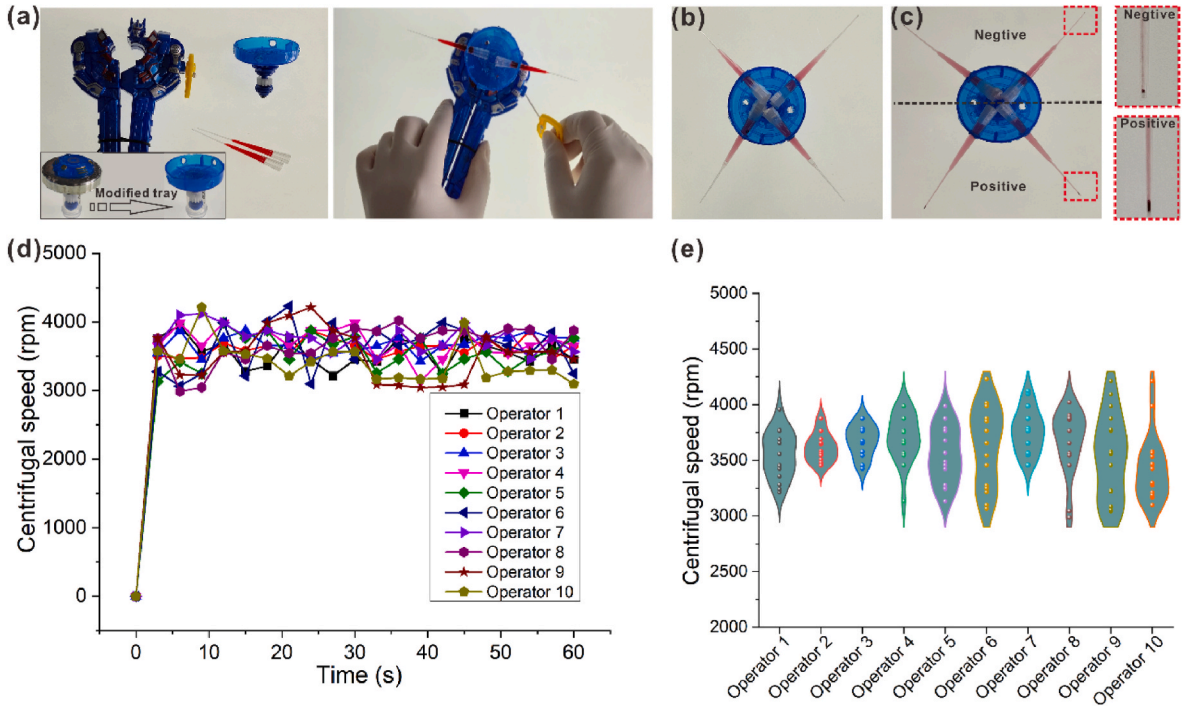

Fig. 2. (a) The centrifugal tray was modified by the commercial pulling-force spinning top. (b–c) Experimental results of before (b) and after centrifugation (c). The concentration of N protein was 100 ng/mL. (d) The centrifugal speeds over time were performed by ten independent individuals. (e) Statistical analysis of velocity in plateau period of ten independent individuals.

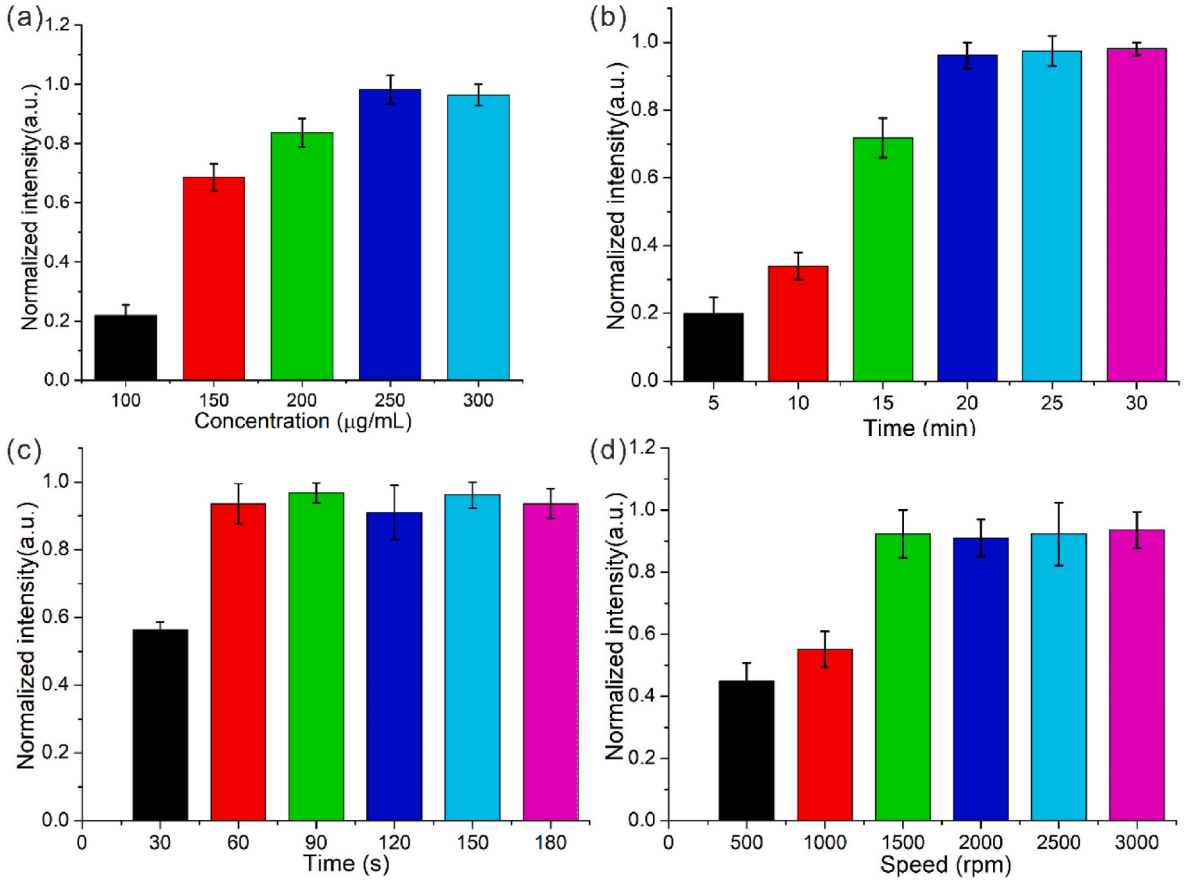

Fig. 3. Optimization of condition in the homogeneous immunoreaction and centrifugal process. (a) The result of immunoreaction under different red latex nanobeads concentration (a), incubation time (b), centrifugation time (c), and centrifugation speed (d).

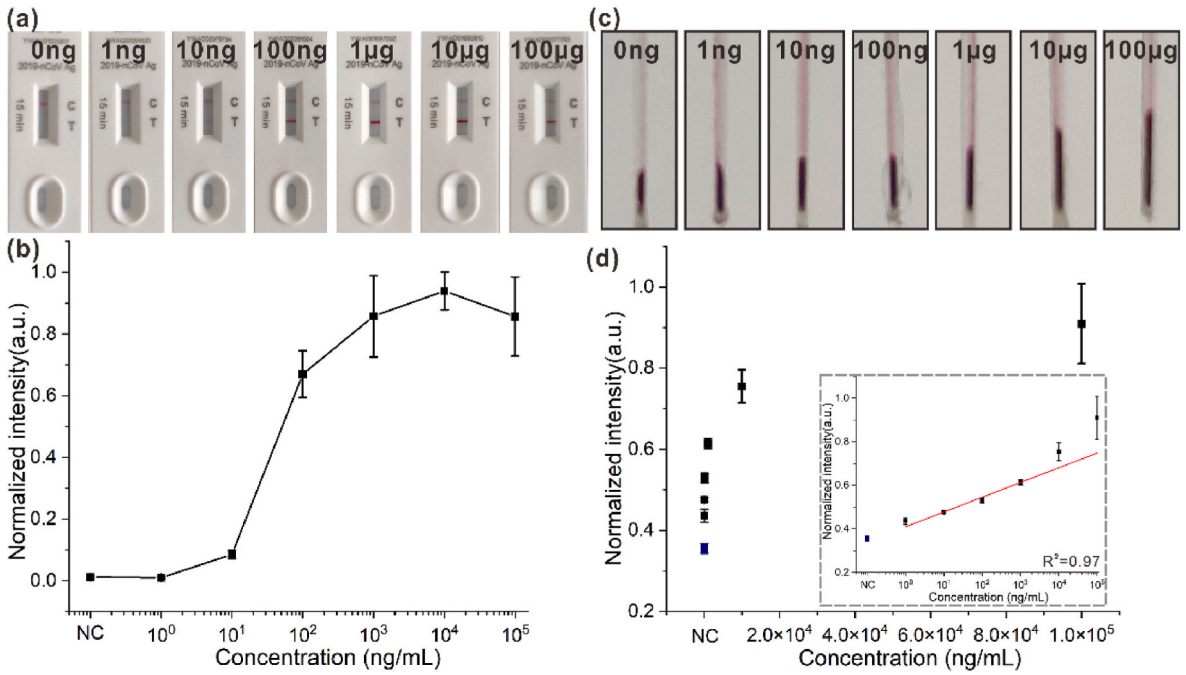

Fig. 4. The sensitivity testing of two systems. (a) The photographic images of the LFIA after loading different concentrations of N protein of SARS-CoV-2. (b) The statistical result of (a), n = 3. (c) The photographic images of the HCM after loading different concentrations of N protein of SARS-CoV-2. (d) The statistical result from HCM of different concentrations of N protein of SARS-CoV-2, n = 3.

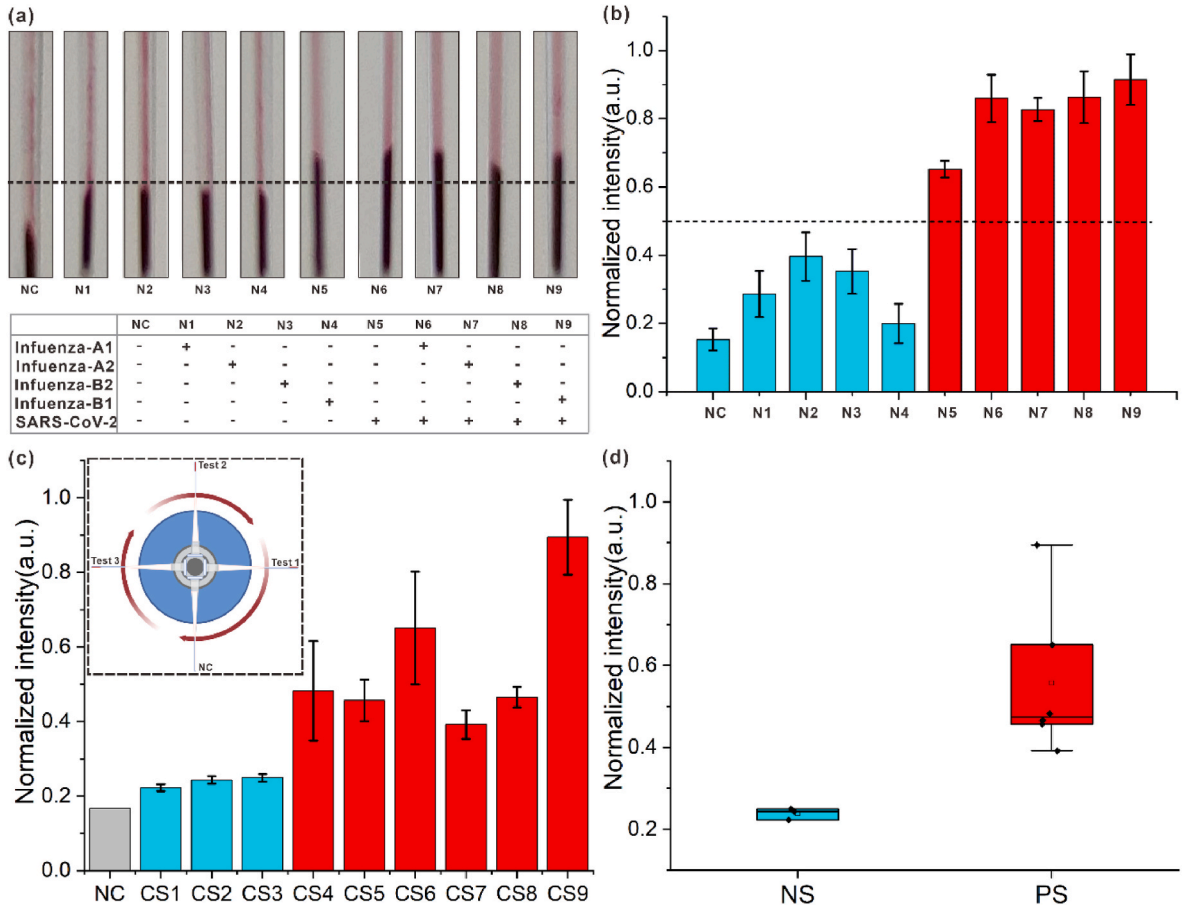

Fig. 5. (a–b) The photographic images and corresponding statistical results (b) of the HCM after loading different samples (n = 3). (c) The results of the HCM for clinical samples. CS1-CS4 indicates clinical negative samples and CS4-CS9 indicates positive clinical samples. Each sample was tested three times. The inset represents a schematic diagram of clinical sample testing on HCM. (d) The statistical results of (c). NS and PS indicate negative and positive samples, respectively.

out directly on a mini tabletop centrifuge by modifying the centrifuge tube and micropipette tip, which can be easily performed in a routine laboratory (Figs. S3d–f). To meet POC testing requirements, a commercial pulling-force spinning top was customized for high throughput loading of the micropipette tip, eliminating the need for electrically charged instruments (Fig. 2a–c and Video S1). The centrifugal speed of the pulling-force spinning top is easily stabilized in the range of 3000–4000 rpm powered by hand drive, which meets our experimental requirements (Fig. 2d–e and Fig. S4).

Supplementary data related to this article can be found at https://doi.org/10.1016/j.talanta.2023.124466.

The key parameters in the homogeneous immunoreaction and subsequent centrifugal process were next investigated. Visual detection is achieved by reading the accumulated distance after simple centrifugation. Since the diameter of the commercial micropipette tip is not uniform (Fig. S1), we quantified the preliminary results with the gray value of the cumulative area instead of the cumulative distance. As shown in Fig. 3a–d, the optimal experimental conditions were determined to be 250 μg/mL of red latex nanobeads, 20 min incubation time, and 60-s centrifugation at 1500 rpm. Benefitting from the all-in-one homogeneous immunoreaction and portable visual reading, the analysis can be completed within half an hour, which is significantly shorter than the standard ELISA method. Our HCM provides a distance-based quantitative result, which can be more accurate than other commercially available SARS-CoV-2 POCT kits, providing only semi-quantitative and user-biased readouts based on color intensity.

To verify the sensitivity and reliability of our platform, we simultaneously compared the proposed HCM with conventional LFIA by tenfold series dilutions of samples in PBS solution. As displayed in Fig. 4, the intensity of signal production showed a corresponding increase with the growing concentration of nucleocapsid protein (N) of SARS-CoV-2 ranging from 0 to 100 μg/mL. There is a weak signal from the LFIA when the concentration is 10 ng/mL, while no visible signal was observed at 1 ng/mL (Fig. 4a–b). Importantly, the lowest detection concentration of our free-instrument HCM was determined to be 1 ng/mL, with a dynamic range from 1 to 10 μg/mL (Fig. 4c–d). Conceivably, the detection limit and sensitivity can be further improved by reducing the tip's size in the future.

We further investigated the specificity of this approach by testing potential interfering influenza A/B. As shown in Fig. 5a–b, the interfering influenzas (10 μg/mL) all resulted in shorter accumulation lengths comparable to the negative control sample. A long accumulation length was observed with SARS-CoV-2 of the same concentration, which was about more than two times of other influenzas. Together, these findings suggest that forming longer lengths was due to the specific binding of SARS-CoV-2 spike N protein against antibodies labeled nanoparticles.

To further verify the practicability of this method, we first attempted the application to the mock swab sample. Six nasal swab samples from healthy volunteers with negative results from nucleic acid testing, spiked with 10 μg/mL SARS-CoV-2 N protein, were used as testing samples or with PBS for negative samples. As shown in Figs. S5a–b, the results demonstrated that our method can still distinguish positive and negative samples successfully, indicating no interference with the results from the nasal secretions.

Finally, we evaluated the performance of the optimized HCM method by comparing the results obtained from RT-PCR, LFIA, and HCM testing on nine clinical samples (Fig. 5c). Detailed information regarding clinical samples and their testing results is presented in Table S1. As demonstrated in Fig. 5c–d, all six PCR-confirmed SARS-CoV-2-positive samples (CS5-CS9) yielded a longer agglutination distance than the negative samples (CS2-CS4) (Fig. 5c). Furthermore, the statistical result indicates a significant differentiation between negative and positive samples (Fig. 5d). These results demonstrate the clinical potential of the proposed HCM technology, particularly in low-resource settings.

3. Conclusion

In summary, our proposed method offers many practical advantages: 1) no washing due to on-pot homogeneous reaction, 2) just needs commercial micropipette-tip avoiding complicated processing, 3) low cost for one test (<$0.1/test), 4) testing on a hand-powered centrifugal toy, no instrumentation required, 5) distance-based naked eye reading, no optical equipment required, 6) massive parallelization for multiple testing. Despite the obvious advantages, there remains significant room for improvement: 1) Based on the versatility of the platform, the antigen or antibody can be easily replaced for other virus detection, 2) Integration of the whole blood separation module to achieve serological immune detection, 3) Integration of liquid distribution module to realize simultaneous detection of multiple targets in a single sample [29]. Due to the non-uniform diameter of commercial micropipette tips, we quantified the results using the gray value of the cumulative area rather than the cumulative distance. Alternatively, the assay can be quantitatively scored using image analysis, including automated smartphone-based approaches. Additionally, producing micropipette tips with uniform diameter through injection molding or soft lithography can further improve the accuracy of our results. Overall, we have represented a simple-step immunoassay with a centrifugal micropipette-tip design for portable quantitative self-testing of the SARS-CoV-2 Virus, which will have broad applications in POCTs, especially in rural areas where laboratory equipment and resources are scarce.

Credit author statement

Chungen Qian: Investigation, Conceptualization, Writing – original draft, Editing. Jiashuo Li: Writing – original draft, Editing. Zheng Pang: Writing – original draft, Editing. Han Xie: Software, Visualization, Editing. Chao Wan: Software, Visualization, Editing. Shunji Li: Visualization, Editing. Xin Wang: Software, Visualization, Editing. Yujin Xiao: Software, Visualization. Xiaojun Feng: Visualization, Editing. Yiwei Li: Visualization, Editing. Peng Chen: Conceptualization, Supervision, Writing- Reviewing and Editing. Bi-Feng Liu: Conceptualization, Supervision, Writing- Reviewing and Editing.

Declaration of competing interest

The authors declare that they have no known competing financial interests or personal relationships that could have appeared to influence the work reported in this paper.

Data availability

Data will be made available on request.

Acknowledgments

The authors gratefully acknowledge the financial supports from the National Key Research and Development Program of China (2021YFA1101500), the National Natural Science Foundation of China (22074047), and the Fundamental Research Funds for Central Universities, HUST (2020kfyXJJS034). We also thank the software tool BioRender (http://www.biorender.com/) to offer some of the elements of graphic.

Appendix A. Supplementary data

Supplementary data to this article can be found online at https://doi.org/10.1016/j.talanta.2023.124466.

References

[1] E. Callaway, How months-long COVID infections could seed dangerous new variants, Nature 606 (7914) (2022) 452–455, https://doi.org/10.1038/d41586-022-01613-2.

[2] E. Topol, It's not too late, Science 375 (6578) (2022) 245, https://doi.org/10.1126/science.abo1074.

[3] F. Wu, S. Zhao, B. Yu, Y.M. Chen, W. Wang, Z.G. Song, Y. Hu, Z.W. Tao, J.H. Tian, Y.Y. Pei, M.L. Yuan, Y.L. Zhang, F.H. Dai, Y. Liu, Q.M. Wang, J.J. Zheng, L. Xu, E. C. Holmes, Y.Z. Zhang, A new coronavirus associated with human respiratory disease in China, Nature 579 (7798) (2020) 265–269, https://doi.org/10.1038/s41586-020-2008-3.

[4] O. Filchakova, D. Dossym, A. Ilyas, T. Kuanysheva, A. Abdizhamil, R. Bukasov, Review of COVID-19 testing and diagnostic methods, Talanta 244 (2022), 123409, https://doi.org/10.1016/j.talanta.2022.123409.

[5] D. Najjar, J. Rainbow, S. Sharma Timilsina, P. Jolly, H. de Puig, M. Yafia, N. Durr, H. Sallum, G. Alter, J.Z. Li, X.G. Yu, D.R. Walt, J.A. Paradiso, P. Estrela, J.J. Collins, D.E. Ingber, A lab-on-a-chip for the concurrent electrochemical detection of SARS-CoV-2 RNA and anti-SARS-CoV-2 antibodies in saliva and plasma, Nat Biomed Eng 6 (8) (2022) 968–978, https://doi.org/10.1038/s41551-022-00919-w.

[6] Z. Lin, J. Zhang, Z. Zou, G. Lu, M. Wu, L. Niu, Y. Zhang, A dual-encoded bead-based immunoassay with tunable detection range for COVID-19 serum evaluation, Angew Chem. Int. Ed. Engl. 61 (37) (2022), e202203706, https://doi.org/10.1002/anie.202203706.

[7] M. Broto, M.M. Kaminski, C. Adrianus, N. Kim, R. Greensmith, S. Dissanayake-Perera, A.J. Schubert, X. Tan, H. Kim, A.S. Dighe, J.J. Collins, M.M. Stevens, Nanozyme-catalysed CRISPR assay for preamplification-free detection of non-coding RNAs, Nat. Nanotechnol. 17 (10) (2022) 1120–1126, https://doi.org/10.1038/s41565-022-01179-0.

[8] X. Wang, X.Z. Hong, Y.W. Li, Y. Li, J. Wang, P. Chen, B.F. Liu, Microfluidics-based strategies for molecular diagnostics of infectious diseases, Mil Med Res 9 (1) (2022) 11, https://doi.org/10.1186/s40779-022-00374-3.

[9] A.N. Grossberg, L.A. Koza, A. Ledreux, C. Prusmack, H.K. Krishnamurthy, V. Jayaraman, A.C. Granholm, D.A. Linseman, A multiplex chemiluminescent immunoassay for serological profiling of COVID-19-positive symptomatic and asymptomatic patients, Nat. Commun. 12 (1) (2021) 740, https://doi.org/10.1038/s41467-021-21040-7.

[10] Z. Zhu, X. Ma, L. Zhu, Q. Luo, N. Lin, Z. Chen, X. Zhao, Z. Lin, Z. Cai, Equipment-free, gold nanoparticle based semiquantitative assay of SARS-CoV-2-S1RBD IgG from fingertip blood: a practical strategy for on-site measurement of COVID-19 antibodies, Talanta 246 (2022), 123498, https://doi.org/10.1016/j.talanta.2022.123498.

[11] L. Chen, G. Zhang, L. Liu, Z. Li, Emerging biosensing technologies for improved diagnostics of COVID-19 and future pandemics, Talanta 225 (2021), 121986, https://doi.org/10.1016/j.talanta.2020.121986.

[12] C.J. Potter, Y. Hu, Z. Xiong, J. Wang, E. McLeod, Point-of-care SARS-CoV-2 sensing using lens-free imaging and a deep learning-assisted quantitative agglutination assay, Lab Chip 22 (19) (2022) 3744–3754, https://doi.org/10.1039/d2lc00289b.

[13] S. Esmail, M.J. Knauer, H. Abdoh, C. Voss, B. Chin-Yee, P. Stogios, A. Seitova, A. Hutchinson, F. Yusifov, T. Skarina, E. Evdokimova, S. Ackloo, L. Lowes, B. D. Hedley, V. Bhayana, I. Chin-Yee, S.S. Li, Rapid and accurate agglutination-based testing for SARS-CoV-2 antibodies, Cell Rep Methods 1 (2) (2021), 100011, https://doi.org/10.1016/j.crmeth.2021.100011.

[14] H. Tong, C. Cao, M. You, S. Han, Z. Liu, Y. Xiao, W. He, C. Liu, P. Peng, Z. Xue, Y. Gong, C. Yao, F. Xu, Artificial intelligence-assisted colorimetric lateral flow immunoassay for sensitive and quantitative detection of COVID-19 neutralizing antibody, Biosens. Bioelectron. 213 (2022), 114449, https://doi.org/10.1016/j.bios.2022.114449.

[15] J. Xu, W. Suo, Y. Goulev, L. Sun, L. Kerr, J. Paulsson, Y. Zhang, T. Lao, Handheld microfluidic filtration platform enables rapid, low-cost, and robust self-testing of SARS-CoV-2 virus, Small 17 (52) (2021), e2104009, https://doi.org/10.1002/smll.202104009.

[16] M. Wu, S. Wu, G. Wang, W. Liu, L.T. Chu, T. Jiang, H.K. Kwong, H.L. Chow, I.W. S. Li, T.H. Chen, Microfluidic particle dam for direct visualization of SARS-CoV-2 antibody levels in COVID-19 vaccinees, Sci. Adv. 8 (22) (2022), eabn6064, https://doi.org/10.1126/sciadv.abn6064.

[17] H. Yuan, P. Chen, C. Wan, Y. Li, B.F. Liu, Merging microfluidics with luminescence immunoassays for urgent point-of-care diagnostics of COVID-19, Trends Anal. Chem. 157 (2022), 116814, https://doi.org/10.1016/j.trac.2022.116814.

[18] Y. Li, Y. Ma, X. Jiao, T. Li, Z. Lv, C.J. Yang, X. Zhang, Y. Wen, Control of capillary behavior through target-responsive hydrogel permeability alteration for sensitive visual quantitative detection, Nat. Commun. 10 (1) (2019) 1036, https://doi.org/10.1038/s41467-019-08952-1.

[19] M.F. Abate, S. Jia, M.G. Ahmed, X. Li, L. Lin, X. Chen, Z. Zhu, C. Yang, Visual quantitative detection of circulating tumor cells with single-cell sensitivity using a portable microfluidic device, Small 15 (14) (2019), e1804890, https://doi.org/10.1002/smll.201804890.

[20] Y. Li, J. Xuan, Y. Song, W. Qi, B. He, P. Wang, L. Qin, Nanoporous glass integrated in volumetric bar-chart chip for point-of-care diagnostics of non-small cell lung cancer, ACS Nano 10 (1) (2016) 1640–1647, https://doi.org/10.1021/acsnano.5b07357.

[21] Y. Song, X. Xia, X. Wu, P. Wang, L. Qin, Integration of platinum nanoparticles with a volumetric bar-chart chip for biomarker assays, Angew Chem. Int. Ed. Engl. 53 (46) (2014) 12451–12455, https://doi.org/10.1002/anie.201404349.

[22] X. Liu, Y. Wang, Y. Song, Visually multiplexed quantitation of heavy metal ions in water using volumetric bar-chart chip, Biosens. Bioelectron. 117 (2018) 644–650, https://doi.org/10.1016/j.bios.2018.06.046.

[23] Y. Song, Y. Zhang, P.E. Bernard, J.M. Reuben, N.T. Ueno, R.B. Arlinghaus, Y. Zu, L. Qin, Multiplexed volumetric bar-chart chip for point-of-care diagnostics, Nat. Commun. 3 (2012) 1283, https://doi.org/10.1038/ncomms2292.

[24] F. Gong, H.X. Wei, J. Qi, H. Ma, L. Liu, J. Weng, X. Zheng, Q. Li, D. Zhao, H. Fang, L. Liu, H. He, C. Ma, J. Han, A. Sun, B. Wang, T. Jin, B. Li, B. Li, Pulling-force spinning top for serum separation combined with paper-based microfluidic devices in COVID-19 ELISA diagnosis, ACS Sens. 6 (7) (2021) 2709–2719, https://doi.org/10.1021/acssensors.1c00773.

[25] M.S. Bhamla, B. Benson, C. Chai, G. Katsikis, A. Johri, M. Prakash, Hand-powered ultralow-cost paper centrifuge, Nature Biomedical Engineering 1 (1) (2017).

[26] I. Michael, D. Kim, O. Gulenko, S. Kumar, S. Kumar, J. Clara, D.Y. Ki, J. Park, H. Y. Jeong, T.S. Kim, S. Kwon, Y.K. Cho, A fidget spinner for the point-of-care diagnosis of urinary tract infection, Nat Biomed Eng 4 (6) (2020) 591–600, https://doi.org/10.1038/s41551-020-0557-2.

[27] Y. Song, Y. An, W. Liu, W. Hou, X. Li, B. Lin, Z. Zhu, S. Ge, H.H. Yang, C. Yang, Centrifugal micropipette-tip with pressure signal readout for portable quantitative detection of myoglobin, Chem. Commun. 53 (86) (2017) 11774–11777, https://doi.org/10.1039/c7cc07231g.

[28] B.L. Thompson, Y. Ouyang, G.R. Duarte, E. Carrilho, S.T. Krauss, J.P. Landers, Inexpensive, rapid prototyping of microfluidic devices using overhead transparencies and a laser print, cut and laminate fabrication method, Nat. Protoc. 10 (6) (2015) 875–886, https://doi.org/10.1038/nprot.2015.051.

[29] Y. Xiao, S. Li, Z. Pang, C. Wan, L. Li, H. Yuan, X. Hong, W. Du, X. Feng, Y. Li, P. Chen, B.F. Liu, Multi-reagents dispensing centrifugal microfluidics for point-of-care testing, Biosens. Bioelectron. 206 (2022), 114130, https://doi.org/10.1016/j.bios.2022.114130.